

## REPORT DOCUMENTATION PAGE

*Form Approved  
OMB No. 0704-0188*

The public reporting burden for this collection of information is estimated to average 1 hour per response, including the time for reviewing instructions, searching existing data sources, gathering and maintaining the data needed, and completing and reviewing the collection of information. Send comments regarding this burden estimate or any other aspect of this collection of information, including suggestions for reducing the burden, to Department of Defense, Washington Headquarters Services, Directorate for Information Operations and Reports (O704-0188), 1215 Jefferson Davis Highway, Suite 1204, Arlington, VA 22202-4302. Respondents should be aware that notwithstanding any other provision of law, no person shall be subject to any penalty for failing to comply with a collection of information if it does not display a currently valid OMB control number.

**PLEASE DO NOT RETURN YOUR FORM TO THE ABOVE ADDRESS.**

1. REPORT DATE (DD-MM-YYYY) Nov 24, 2004			2. REPORT TYPE FINAL		3. DATES COVERED (From - To) From 5/17/04 to 11/24/04		
4. TITLE AND SUBTITLE  MIMO Based Eigen-Space Spreading			5a. CONTRACT NUMBER N00014-04-M-0161  5b. GRANT NUMBER  5c. PROGRAM ELEMENT NUMBER  5d. PROJECT NUMBER  5e. TASK NUMBER  5f. WORK UNIT NUMBER				
6. AUTHOR(S) Ahmed Eltawil Babak Daneshrad			8. PERFORMING ORGANIZATION REPORT NUMBER PUL006				
7. PERFORMING ORGANIZATION NAME(S) AND ADDRESS(ES) Pulsar Communication Systems 3862 Kim Lane Encino, CA 91436			9. SPONSORING/MONITORING AGENCY NAME(S) AND ADDRESS(ES) Dr. Philemon Johnson, Dr. Santanu Das, Dr. Joel Davis Office of Naval Research 800 North Quincy St. Arlington, VA 22217-5660				
10. SPONSOR/MONITOR'S ACRONYM(S)			11. SPONSOR/MONITOR'S REPORT NUMBER(S)				
12. DISTRIBUTION/AVAILABILITY STATEMENT Approved for public release; distribution unlimited.							
13. SUPPLEMENTARY NOTES							
14. ABSTRACT  In this work, Pulsar leveraged the multiple input multiple output (MIMO) concept to achieve anti-jamming and low probability of detection/interception (AJ/LPI/LPD) communications. The proposed work randomizes the signal in space, as well as time and frequency. Space randomization will be achieved by transmitting on the spatial singularities of the MIMO matrix channel. Combination of this powerful technique with orthogonal frequency division multiplexing (OFDM) based modulation and traditional time and frequency spreading techniques results in a highly secure mode of communications. The results show that for LPD, almost 20 dB reduction in overall TX power can be achieved for the same performance at 5% outage when going from a single antenna system to an 8 antenna system. Moreover, our results show that the eigen vector spreading concept is complementary and additive to conventional spread spectrum techniques such as frequency hopped spread spectrum and direct sequence spread spectrum							
15. SUBJECT TERMS Wireless Communicatons; OFDM, Multi-Antenna Systems, Spread Spectrum							
16. SECURITY CLASSIFICATION OF: a. REPORT Unclassified			17. LIMITATION OF ABSTRACT UU		18. NUMBER OF PAGES 23	19a. NAME OF RESPONSIBLE PERSON Babak Daneshrad  19b. TELEPHONE NUMBER (Include area code) (310) 738-1787	

## INSTRUCTIONS FOR COMPLETING SF 298

- 1. REPORT DATE.** Full publication date, including day, month, if available. Must cite at least the year and be Year 2000 compliant, e.g. 30-06-1998; xx-06-1998; xx-xx-1998.
- 2. REPORT TYPE.** State the type of report, such as final, technical, interim, memorandum, master's thesis, progress, quarterly, research, special, group study, etc.
- 3. DATES COVERED.** Indicate the time during which the work was performed and the report was written, e.g., Jun 1997 - Jun 1998; 1-10 Jun 1996; May - Nov 1998; Nov 1998.
- 4. TITLE.** Enter title and subtitle with volume number and part number, if applicable. On classified documents, enter the title classification in parentheses.
- 5a. CONTRACT NUMBER.** Enter all contract numbers as they appear in the report, e.g. F33615-86-C-5169.
- 5b. GRANT NUMBER.** Enter all grant numbers as they appear in the report, e.g. AFOSR-82-1234.
- 5c. PROGRAM ELEMENT NUMBER.** Enter all program element numbers as they appear in the report, e.g. 61101A.
- 5d. PROJECT NUMBER.** Enter all project numbers as they appear in the report, e.g. 1F665702D1257; ILIR.
- 5e. TASK NUMBER.** Enter all task numbers as they appear in the report, e.g. 05; RF0330201; T4112.
- 5f. WORK UNIT NUMBER.** Enter all work unit numbers as they appear in the report, e.g. 001; AFAPL30480105.
- 6. AUTHOR(S).** Enter name(s) of person(s) responsible for writing the report, performing the research, or credited with the content of the report. The form of entry is the last name, first name, middle initial, and additional qualifiers separated by commas, e.g. Smith, Richard, J, Jr.
- 7. PERFORMING ORGANIZATION NAME(S) AND ADDRESS(ES).** Self-explanatory.
- 8. PERFORMING ORGANIZATION REPORT NUMBER.** Enter all unique alphanumeric report numbers assigned by the performing organization, e.g. BRL-1234; AFWL-TR-85-4017-Vol-21-PT-2.
- 9. SPONSORING/MONITORING AGENCY NAME(S) AND ADDRESS(ES).** Enter the name and address of the organization(s) financially responsible for and monitoring the work.
- 10. SPONSOR/MONITOR'S ACRONYM(S).** Enter, if available, e.g. BRL, ARDEC, NADC.
- 11. SPONSOR/MONITOR'S REPORT NUMBER(S).** Enter report number as assigned by the sponsoring/monitoring agency, if available, e.g. BRL-TR-829; -215.
- 12. DISTRIBUTION/AVAILABILITY STATEMENT.** Use agency-mandated availability statements to indicate the public availability or distribution limitations of the report. If additional limitations/ restrictions or special markings are indicated, follow agency authorization procedures, e.g. RD/FRD, PROPIN, ITAR, etc. Include copyright information.
- 13. SUPPLEMENTARY NOTES.** Enter information not included elsewhere such as: prepared in cooperation with; translation of; report supersedes; old edition number, etc.
- 14. ABSTRACT.** A brief (approximately 200 words) factual summary of the most significant information.
- 15. SUBJECT TERMS.** Key words or phrases identifying major concepts in the report.
- 16. SECURITY CLASSIFICATION.** Enter security classification in accordance with security classification regulations, e.g. U, C, S, etc. If this form contains classified information, stamp classification level on the top and bottom of this page.
- 17. LIMITATION OF ABSTRACT.** This block must be completed to assign a distribution limitation to the abstract. Enter UU (Unclassified Unlimited) or SAR (Same as Report). An entry in this block is necessary if the abstract is to be limited.

---

## MIMO Based Eigen-Space Spreading

**Nov. 24<sup>th</sup>, 2004**

**Office of Naval Research (ONR)**

***Issued by the U.S. Office of Naval Research Under***

***Contract No. N00014-04-M-0161***

Name of Contractor: **Pulsar Communication Systems**

Project Scientist: **Dr. Babak Daneshrad**

Business Address:

**3862 Kim Ln.**

**Encino, CA 91436**

Phone Number: **(310) 738-1787**

Effective Date: **May 17, 2004**

Short Title of Work: **MIMO Based Eigen-Space Spreading**

Contract Expiration Date: **Nov 24, 2004**

Reporting Period: **05/17/04 – 11/24/04**

### ***Disclaimer***

The views and conclusions contained in this document are those of the authors and should not be interpreted as representing the official policies, either express or implied, of the Defense Advanced Research Projects Agency or the U.S. Government.

### ***UNCLASSIFIED***

Approved for public release; distribution unlimited

## 1. Introduction

This final report presents Pulsar's progress during the course of the Phase-1 NAVY SBIR topic: N04-108, TITLE: MIMO Based Eigen-Space Spreading. The report will present the findings, as well as a description of future work to be undertaken as part of a possible phase-2 effort. In our proposal, Pulsar leveraged the multiple input multiple output (MIMO) concept to achieve anti-jamming and low probability of detection/interception (AJ/LPI/LPD) communications. The proposed work randomizes the signal in space, as well as time and frequency. Space randomization will be achieved by transmitting on the spatial eigenvectors of the MIMO matrix channel. Combination of this powerful technique with orthogonal frequency division multiplexing (OFDM) based modulation and traditional time and frequency spreading techniques results in a revolutionary secure mode of communications.

The results to date are quite encouraging. As is shown in Table 1, in the case of LPD protection, we see that for an outage of 5% (95% coverage), the same data rate could be transmitted with almost 20 dB less power when the transmitter and receiver are outfitted with 8 antenna elements. Moreover, our results show that the eigen vector spreading concept is complementary and additive to conventional spread spectrum techniques such as frequency hopped spread spectrum and direct sequence spread spectrum.

MIMO Configuration	95% Capacity at 20 dB SNR	Required SNR to achieve 1 bps/Hz of Capacity at 95%
1x1	2.6 bps/Hz	12.8 dB
2x2	8.0 bps/Hz	1.2 dB
4x4	19.0 bps/Hz	-4.9 dB
8x8	40.8 bps/Hz	-9.3 dB

Table 1, Effectiveness of MIMO spatial multiplexing in increasing throughput or improving LPD

In this report we summarize the progress during the course of this phase-1 effort. Section 2 provides an overview of the proposed system architecture and the underlying principals of Eigen Space Spreading. Section 3 outlines a comprehensive simulation environment that incorporates the geographical location of scattering elements and their relationship to the eigenvectors of the channel. Section 4 presents results from a study whereby the effectiveness of Eigne space spreading was evaluated for LPD communications. Finally Section 5 outlines strategies for achieving AJ and LPI capability. The report also includes an Appendix that discusses singular value decomposition which is the main theory behind the identification of the eigenvectors.

## 2. System Overview

Pulsar is proposing to use the spatial characteristics of a MIMO channel to enable a higher degree of data security [1],[2]. Fundamentally, a MIMO wireless system consists of  $M_T$  transmit antennas and  $M_R$  receive antennas whereas traditional systems only use a single transmit and a single receive antenna. Figure 1 illustrates such a system. The multiplicity of transmit and receive antennas could be used in the traditional beamforming (smart antenna) mode, or in the newly proposed eigen-space (spatial) multiplexing mode which we define as the default MIMO mode. In the default MIMO mode, the transmitted data stream is multiplexed on the  $M_T$  transmit antennas. This forces different data to be sent out of each antenna. The receiver uses the signal observed at the  $M_R$  receive antennas and performs MIMO matrix inversion to recover the  $M_T$  independent data streams sent from the transmitter. After de-multiplexing, the original data stream is delivered to the user. In this work, we will exploit the capability of MIMO systems to transmit data on unique eigen-spaces of the channel matrix. When these eigen-spaces are used in parallel the system delivers high throughput rates, when these eigen-spaces are used in a randomized order the systems delivers high fidelity AJ/LPI/LPD waveforms.

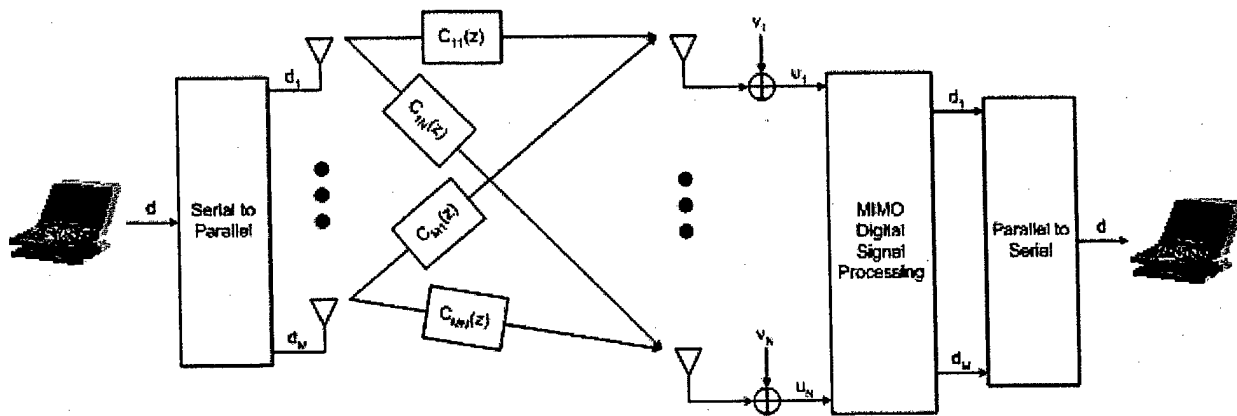


Figure 1 MIMO Basic Concepts

The ultimate goal of a communication system is to maximize the transmission capacity while minimizing the probability of detection/interception and decreasing the jamming sensitivity of the communication. Pulsar is proposing a unique system that combines the power of OFDM modulation to mitigate multipath

and to provide a natural partitioning of the spectrum with multi antenna MIMO techniques that provide for an added signaling dimension for scrambling the data. In the proposed system the transmitter unit scrambles the data using the spatial properties of the communication channel  $H$ . Only a unit which has knowledge of the MIMO communication channel  $H$  is able to correctly decipher the message. Furthermore, the transmitter will maximize the power transmitted along the channel  $H$  and minimize the power transmitted in other directions. This same mechanism reduces the probability of an enemy unit detecting the transmission. The receiver unit also uses MIMO technology to correctly receive and descramble the transmitted signal and performs spatial interference cancellation to provide a high degree of immunity to jammer interference. To better illustrate how the MIMO eigen-space spreading waveform is generated, the reader is referred to

Figure 2. As is shown, the proposed approach allows each individual sub-carrier of the OFDM modulated waveform to be transmitted in the direction of one of the  $N$  randomly chosen eigen-vectors within the eigen-space. OFDM [3],[4] is a mechanism by which a frequency selective channel is divided into a group of orthogonal flat fading channel. The aggregate throughput of the channel is maintained by combining the throughput of each sub-carrier. However, each sub-carrier experiences a flat fading channel and therefore does not require equalization. The top level block diagram of the transmitter and receiver are shown in Figure 3.

In the proposed architecture, the transmitter determines the eigen vector of the MIMO transmission channel  $H$ . The knowledge of  $H$  at the transmitter can be obtained by using the channel reciprocity of a Time Division Duplex (TDD) system or by feedback from the receiver. For each transmitted symbol, the transmitter randomly chooses one of the eigen vectors for transmission. At the receiver, OFDM demodulation is first used to recover the transmitted data on the sub-carriers. After parallel to serial conversion of the OFDM sub-carriers, the data is presented to the MIMO digital signal processing unit to recover the transmitted data streams. The MIMO signal processing unit provides multiple functionalities. It inverts the channel to recover the data transmitted from the different antennas. Finally, it performs eigen vector spatial descrambling.

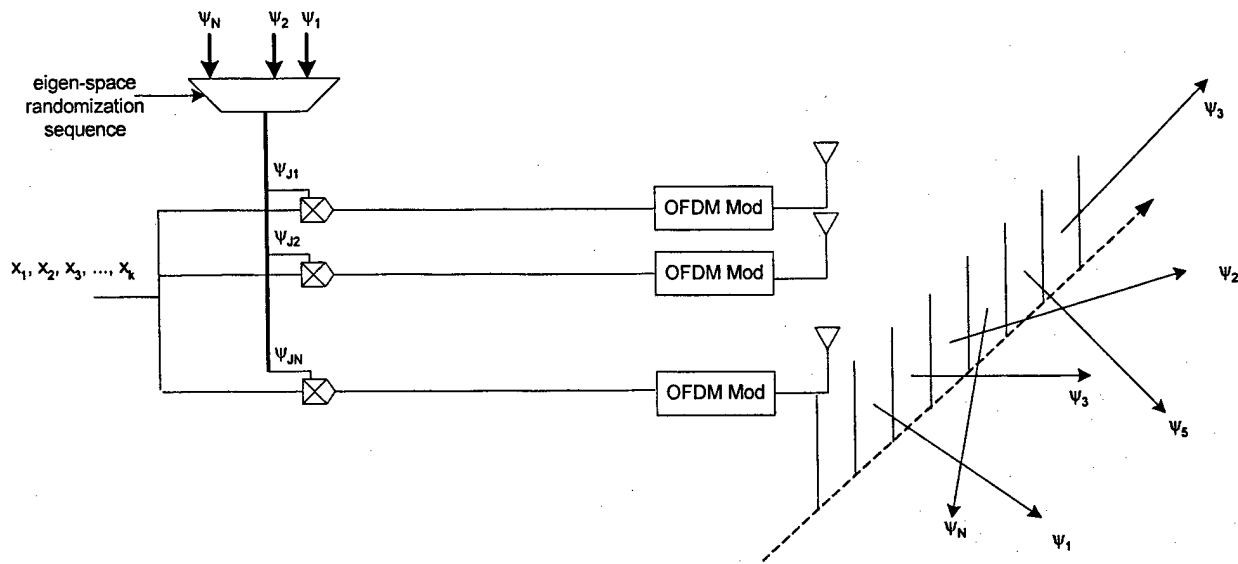


Figure 2 Spatial Scrambling MIMO OFDM Modem Architecture

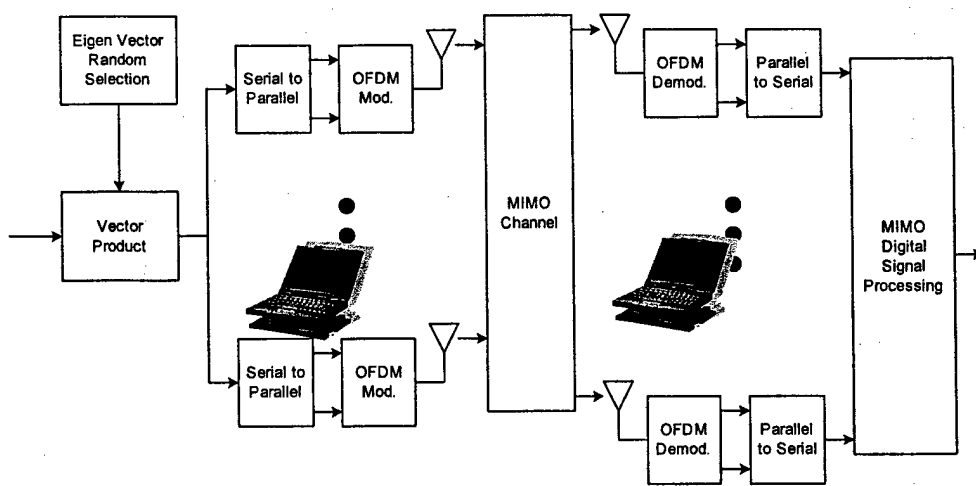


Figure 3 Spatial Scrambling MIMO OFDM Modem Architecture

## OFDM Overview

OFDM is a multi-carrier modulation scheme that has been developed for frequency selective fading channel environments [3]. OFDM modulates the data on orthogonal carriers, which are added and transmitted simultaneously. This effectively divides the wideband channel into a number of narrowband transmission sub-channels. A receiver can therefore be designed using lower complexity narrowband techniques on each sub-channel, which is important for a MIMO system. The use of Discrete Fourier Transform (DFT) for baseband modulation and demodulation allows efficient implementations by making use of the Fast Fourier Transform (FFT).

The OFDM modulator takes a block of  $P$  consecutive symbols  $d(p)$  and performs an inverse DFT (IDFT) to obtain the time domain sequence  $d(t)$  given by:

$$d(t) = \frac{1}{\sqrt{P}} \sum_{p=0}^{P-1} d(p) e^{\frac{j2\pi p}{P} t}$$

A cyclic prefix is then pre-appended to the sequence as illustrated in Figure 4. The last  $L$  symbols of the IDFT output are pre-appended to the front of the IDFT output block. This creates a cyclic guard interval of length  $L$ , which prevents intersymbol (interblock) interference between consecutive OFDM symbols (blocks). The cyclic prefix also ensures orthogonality between sub-carriers when the signal is transmitted over dispersive channels. This guard interval between OFDM symbols must have a length  $L$  greater than the maximum excess delay expected from the channel to eliminate the ISI. Phase transitions at the boundary between consecutive OFDM symbols create spectral re-growth outside the signal bandwidth. To mitigate this effect, windowing of the OFDM symbols should be applied.

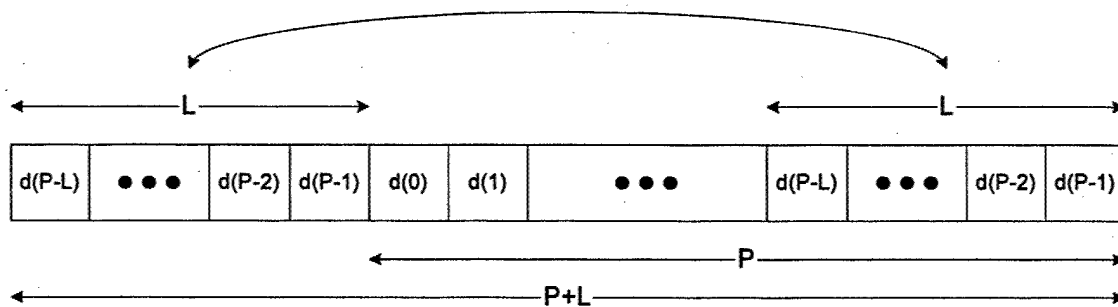


Figure 4. OFDM Cyclic Prefix

At the receiver, the OFDM boundary is identified through the initial synchronization and the first  $L$  symbols of each blocks of  $P+L$  symbols are removed to obtain the sequence of  $P$  symbols  $u(t)$ . These symbols are not corrupted by the previous OFDM symbol (i.e., there is no OFDM symbol ISI) and due to the presence of the cyclic prefix, it can be shown that the sub-carrier orthogonality has been preserved.  $P$

consecutive receive samples  $u(t)$  are then aggregated and sent through a DFT block. The DFT operation yields the channel output  $u(p)$  for each sub-carrier  $p$  as follows:

$$u(p) = \frac{1}{\sqrt{P}} \sum_{t=0}^{P-1} u(t) e^{-j \frac{2\pi p t}{P}}$$

Through the use of the frequency transforms, OFDM divides the broadband signal bandwidth into many orthogonal sub-carrier frequencies, Figure 5. Each orthogonal sub-carrier carries low data rates and can be treated as narrowband systems. The channel is therefore divided in the frequency domain into narrowband channels which allows OFDM to effectively combat harsh multipath propagation environments with a low-level of complexity compared to traditional single carrier equalized QAM schemes or even DSSS based CDMA schemes.

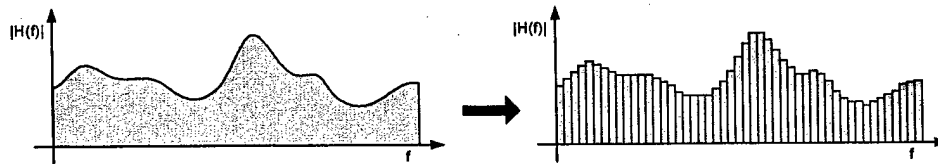


**Figure 5. (left)** A broadband single carrier system suffers from serious frequency selectivity and ISI.  
**(right)** OFDM divides the broadband signal into many smaller subcarriers, each of which sees a flat fading channel with no-ISI.

The number of subcarriers to be used is a function of the signal bandwidth and the coherence bandwidth which is equal to  $B_c = 1/2\pi\tau_{rms}$ , where  $\tau_{rms}$  is the average rms delay spread for the environment. Noting that any two subcarriers that have a separation of less than  $B_c$  are highly correlated, we can simplify some of the receiver processing by exploiting this fact. The channel correlation in the frequency domain can be exploited in OFDM by decreasing the number of sub-carrier transmitting pilots to estimate the channel and using interpolation to compute the channel estimates for the other sub-carriers.

## Channel Singular Value Decomposition (SVD)

The main feature that Pulsar is exploiting is the fact that a MIMO channel  $\mathbf{H}$  can be decomposed into a set of orthogonal eigen modes that are channel dependent. The following discussion explains how a Singular value Decomposition (SVD) [4] technique can be used to obtain these eigen modes.

Consider a system with  $M_T$  antennas at the transmitter and  $M_R$  antennas at the receiver. Transmission is over a Rayleigh flat fading channel (OFDM techniques allow this assumption even when using a wide total aggregate bandwidth by allocating to each sub-carrier a bandwidth that is less than the coherence bandwidth of the channel). Furthermore, assume a transmission vector  $\mathbf{x}$ , a channel matrix  $\mathbf{H}$  and AWGN noise vector  $\mathbf{n}$ . The vector of received symbols can be expressed as:

$$\mathbf{y} = \mathbf{Hx} + \mathbf{n}$$

An SVD analysis of  $\mathbf{H}$  consists of three matrices  $(\mathbf{U}, \mathbf{D}, \mathbf{V})$  where  $\mathbf{U}$  and  $\mathbf{V}$  are unitary matrices and  $\mathbf{D}$  is a diagonal matrix representing the singular values of  $\mathbf{H}$  sorted in descending order. Applying the SVD technique  $\mathbf{H}$  can be expressed as follows:

$$\mathbf{H} = \mathbf{UDV}^*$$

$\mathbf{V}^*$  denotes the transpose conjugate of  $\mathbf{V}$ . The physical meaning of  $\text{SVD}(\mathbf{H})$  is decomposing the channel matrix  $\mathbf{H}$  into a number of independent orthogonal modes of excitation referred to as eigen-modes which we will collectively refer to as the eigen-space. The eigen-space depends on the channel state information (CSI) between a specific transmitter and receiver. For a wireless communication link, the CSI for each transmitter/receiver pair provides a unique channel signature that depends on the channel properties between the pair.

SVD techniques can be exploited in conjunction with MIMO transmission as follows. The transmitter multiplies the signal vector  $\mathbf{x}$  by the matrix  $\mathbf{V}$  prior to sending the signal over the air via  $M_T$  antennas. The receiver multiples the  $M_R$  received signals by the matrix  $\mathbf{U}^*$  as shown in Figure 6. The overall transmission relationship is:

$$\mathbf{y} = \mathbf{U}^*(\mathbf{HVx} + \mathbf{n}) = \mathbf{Dx} + \mathbf{U}^*\mathbf{n}$$

The MIMO channel is thus transformed into parallel SISO channels with non-equal gain where each independent SISO channel is defined by an eigen mode (eigen vector) and its gain is defined by the associated eigen value. Highly secure (LPI/LPD) communication can be established by randomly choosing different eigen modes for each transmission interval. This is possible by weighting the  $\mathbf{V}$  matrix at the transmitter such that only one eigen mode is active per transmission interval. This technique creates a link that is virtually impossible to intercept since the receiver has to posses two pieces of information to be able to correctly demodulate the signal:

- 1- The receiver has to have the accurate CSI. Due to the nature of a wireless channel, this information is unique between any pair of a communication link.
- 2- To demodulate the received signals, the receiver will have to identify which of the active eigen-modes is being used for communication.

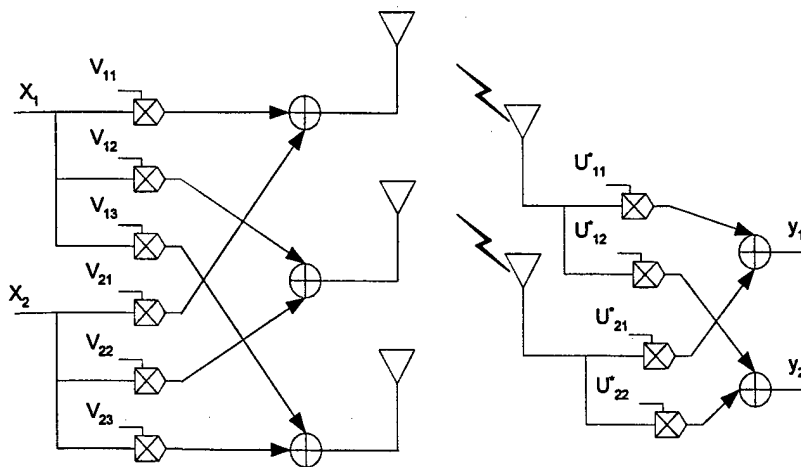


Figure 6 Transmission and Reception of Data Symbols on different Eigen Vectors of the Space

### Analysis of the Minimum Eigen Mode

The minimum eigen value of the MIMO channel  $\mathbf{H}$  is of extreme significance since it specifies the “quality of the channel”. This is strongly linked to what is defined as the “condition number of the matrix”. The condition number is formally defined as the ratio of the maximum eigen value divided by the minimum eigen value of the matrix. The lower this ratio, the better. A low ratio indicates that the eigen modes are well balanced and can handle equivalent loads of data. As this ratio increases, this indicates that the eigen modes are actually not balanced and therefore, it will become extremely difficult to invert the channel, since in reality it is not a true MIMO channel but rather a SISO channel [6].

The minimum eigen value is also a measure of the quality of transmission on a MIMO channel (BER), this is explained by the following analysis [7].

### Adaptive methods to identify SVD modes of the channel

There are many proposed methods to estimate the SVD decomposition of the channel matrix  $\mathbf{H}$ , the simplest being to estimate the channel matrix  $\mathbf{H}$  itself first and then perform SVD analysis to identify the left and right eigen vectors  $\{\mathbf{U}, \mathbf{V}\}$ . However, in a dynamic wireless channel it is not always feasible to assume that channel information is available at both the transmitter and receiver. A majority of algorithms have assumed that  $\mathbf{H}$  is unknown at the transmitter but is known at the receiver through training data (V-blast [8]). This approach however implies an overhead for the training algorithm which leads to a less efficient MIMO system.

A more attractive approach is utilize a two-way data directed technique that will allow both the Tx and the Rx to estimate the left and right singular vectors, without explicitly estimating the channel matrix

first. A study of this approach is presented in [9]. The idea behind this method is to perform a continuous successive estimation of the eigen vectors by employing a feedback scheme in the transmission as follows:

Consider a noiseless TDD system experiencing flat fading expressed by the channel matrix  $H$

$$y^{(i)} = Hx^{(i-1)}$$

$$z^{(i)} = H^T w^{(i)}$$

where  $x^{(i-1)}$  and  $w^{(i-1)}$  are the uplink and downlink data vectors respectively. We can now introduce feedback as follows

$$w^{(i)} = \bar{y}^{(i)}$$

$$x^{(i)} = \bar{z}^{(i)}$$

where the bar (-) indicates complex conjugate without transposing.

Based on this recursion we can write the following equations

$$y^{(i)} = Hx^{(i-1)}$$

$$x^{(i)} = H^* y^{(i)}$$

By applying SVD techniques to the above equations, it can be shown [9] that an iterative approximation of the first eigen modes can be generated as follows

$$y^{(i)} = \sum_k \sigma_k^{(2i-1)} \alpha_k u_k$$

$$x^{(i)} = \sum_k \sigma_k^{(2i)} \alpha_k v_k$$

where  $\sigma$  is the eigen value corresponding to this eigen mode and  $\alpha$  is a constant that depends on the chosen initial data vector  $x^0$ .

This procedure can be repeated for successive eigen modes until all eigen vector have been identified. Figure 7 shows the convergence of the estimated singular pairs for a MIMO channel. The initial singular vector is chosen randomly. In this case two singular modes are estimated for a 3x3 system. The errors for the two singular vectors are averaged and plotted for different SNR values starting from 0 dB up to 20 dB SNR. Part (a) shows the error for the left singular vectors while part (b) shows the errors for the right singular vectors.

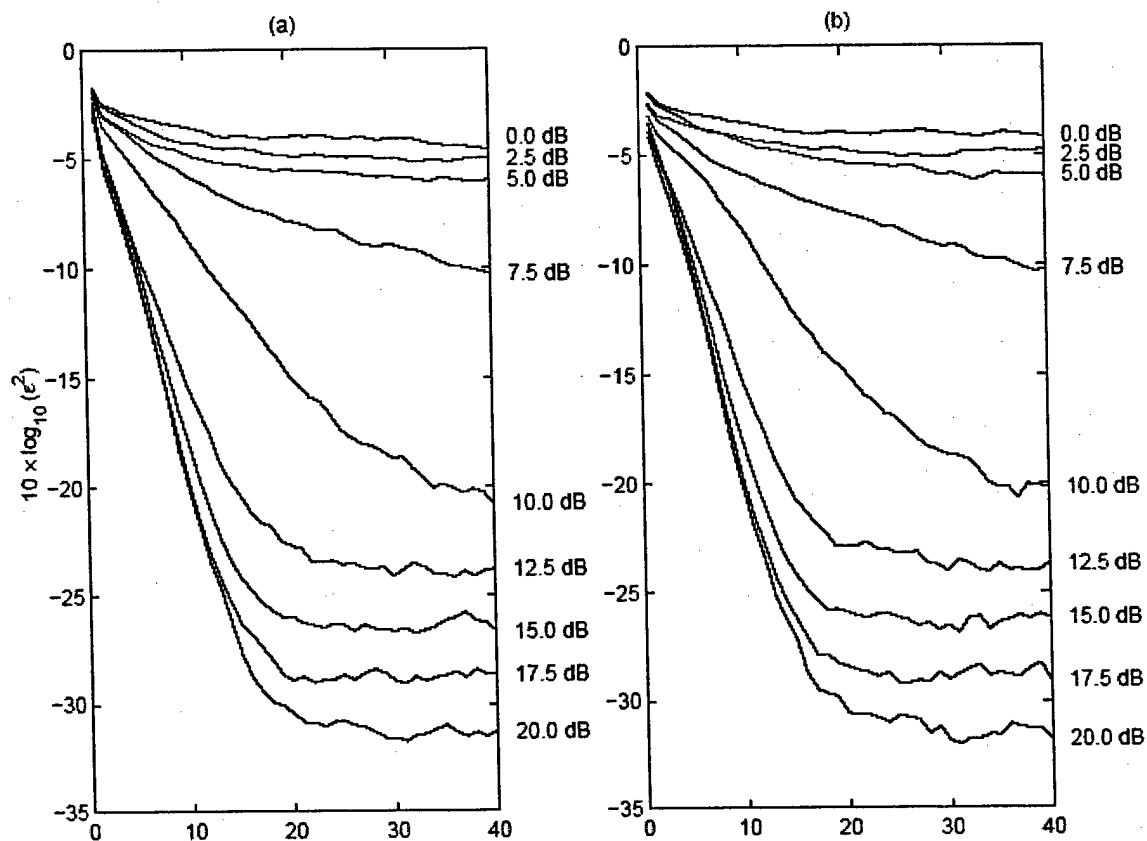


Figure 7 Averaged error across two eigen modes for different SNR settings

### 3. Simulation Environment

This section is devoted to describing the simulation environment that we have developed to properly model the channel. Although there are a number of standard and well accepted approaches for modelling the time domain behaviour of the wireless channel (the most referenced work is that of Saleh and Valenzuela [10]), very few models exist that provide a description of the time and spatial characteristics of the channel. In the proposed work it is important to gain insight into the relationships between the eigen vectors of the channel and the position of the scatters in the environment. As such we have developed a hybrid simulation environment that includes the position of the scattering elements but not their reflection coefficients.

#### *MIMO Channel Model*

We start our discussion by first defining the traditional flat fading channels, where the  $n \times m$  channel matrix is defined by  $\mathbf{H}_{n \times m}$ , where  $n$  is the number of transmit antennas and  $m$  is the number of receive antennas. In this baseline model we assume the elements of the channel matrix to be independent identically distributed complex gaussian random variables. This is a fairly accurate model of an environment consisting of a rich set of uncorrelated scattering elements. In such an environment, the channel matrix is typically of full rank =  $\min(n, m)$ .

In order to migrate this baseline channel model to where it incorporates information about the position of the scatterers we leverage the work reported in the literature. The resulting  $\mathbf{H}$  matrix is given below.

$$\mathbf{H}_{n \times m} = \Psi_{R_{(m \times N_s)}} \Xi_{(N_s \times N_s)} \Psi^T_{T_{(n \times N_s)}}$$

Where the matrix  $\Psi$  consists of the steering vectors from the transmitter or receiver site to the  $N_s$  different scatterers randomly placed in the environment.  $\Psi_R$  is an  $m \times N_s$  matrix of steering vectors from the receiver to the scatterers. Similarly  $\Psi_T$  is  $m \times N_s$  matrix of steering vectors from the transmitter to the  $N_s$  scatterers. The matrix  $\Xi$  is a square  $N_s \times N_s$  matrix of reflection coefficients for each of the scatterers in the environment. Without loss of generality we have chosen a gaussian distribution for the reflection coefficients. If additional information was available about the coefficients, then they could easily be inserted into the  $\Xi$  matrix. With the scatterer information introduced into the channel model, the rank of the channel matrix is now determined by the relative location of the scattering elements. In general, nearby scatterers induce array response vectors that are nearly identical, which means that the rank of the channel is a function of both scatterer location as well as antenna resolution.

With the above formulation of the channel, we now have an effective means of characterizing the interrelationship between the number of scattering elements, their position, their reflection coefficients, and the eigenvalues and eigenvectors of the channel. These will be elaborated on in ensuing subsections. However, before moving on we need to provide the following expression for the total energy of the channel.

$$\sum_{i=1}^r \lambda_i = \text{trace}(\mathbf{H}\mathbf{H}^H) = \text{trace}(\mathbf{H}^H\mathbf{H}) = \|\mathbf{H}\|_F^2$$

Recall that the eigen values  $\lambda_i$  are elements of the diagonal matrix  $\mathbf{D}$  arrived at through the singular value decomposition of the channel matrix  $\mathbf{H}$ . We will use the expression for the trace of a matrix and the eigen modes at both the transmitter and receiver in the discussions that follow.

### Eigen Value Distribution

Figure 8 shows the cumulative distribution functions for the eigen value spread of a 4x4 channel matrix. The CDFs were generated by measuring the eigen values of 1000 unique instances of the Rayleigh channel matrix and the scatterer based channel matrix assuming 10 scattering elements in the

environment. The plot on the left shows the distribution of the Rayleigh channel. It can be seen that the eigenvalues in a Rayleigh based channel are more densely packed than the ones in the scatterer based model. This signifies that there is no dominant eigen mode in these channels. Rather, all directions are more or less equivalent. On the other hand it can be seen from the scatterer based model that in a majority of the channels, there is a single strong mode for transmission. The other modes are all clustered together similar to the Rayleigh based model. Knowledge of this indicates that transmission on the strongest mode will provide us with more bang for the buck than in the case where all eigen modes are equally strong.

In other studies our results indicate that as the number of scattering elements is increased the scatterer based channel characteristics converge to those of the Rayleigh based model. Conversely as the number of scatterers is reduced the relative strength of the strongest eigen mode to the others increases.

In a series of other studies we investigated the relationship of the eigenvectors of the channel to the position of the scattering elements. Figure 9 shows the plot of the two strongest eigen modes as if they were steering vectors. In the figure the + signs correspond to the position of the scattering elements used in this simulation. It is interesting to note that the eigen modes (eigenvectors) point directly at the scattering elements. This is intuitively expected since the only way by which a signal can go from the transmitter to the receiver is by being deflected off of a scattering element.

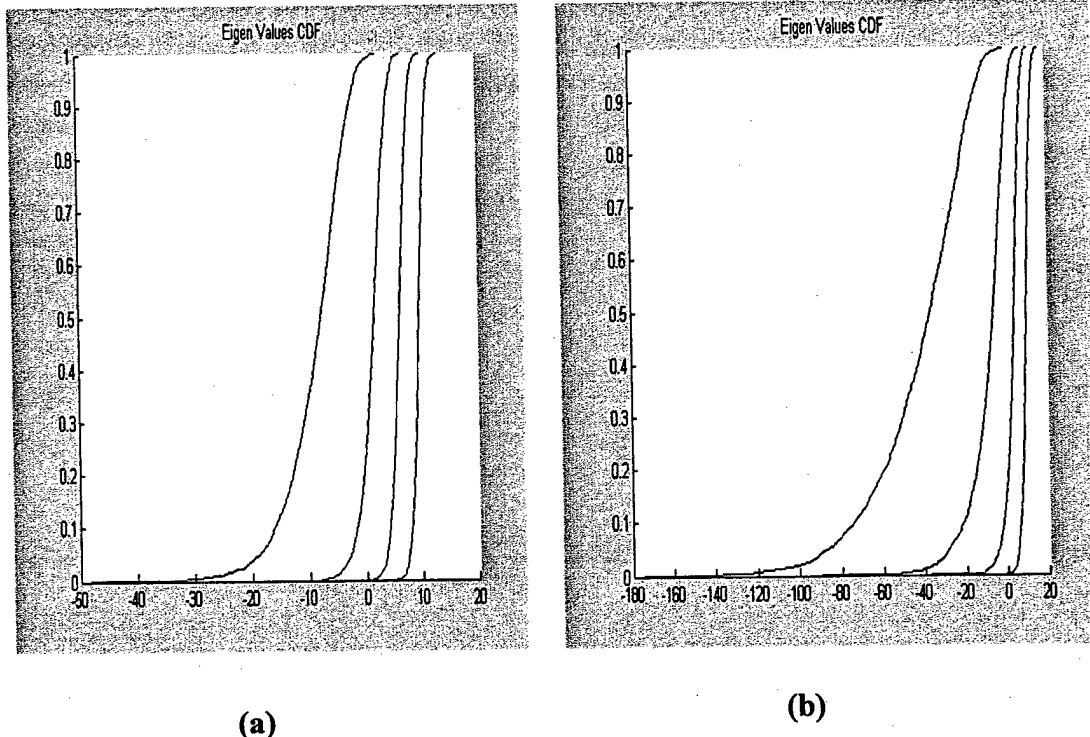


Figure 8 Eigne value distribution of (a) a 4x4 Rayleigh channel matrix; (b) a 4x4 scatterer based channel with 10 randomly placed scattering elements.

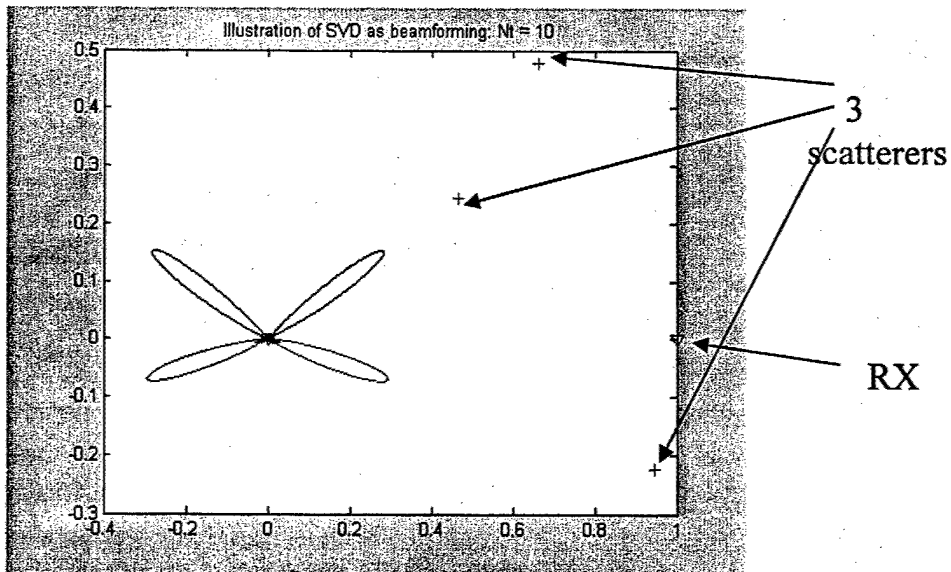


Figure 9 SVD beamforming at the Transmitter

Figure 10 shows the plot of the eigen modes at the receiver assuming the same three scatterers as in Figure 9 above. As in the case of the transmitter, it is clear that the eigenvectors are attempting to point the effective antenna pattern in the direction of the scatterers. It is interesting to note that a simple beamforming approach would not be effective in this situation as creating a beam in the general direction of the transmitter (or receiver) in a scatter rich environment is not the same as doing this in free space. In a scatter rich environment, the actual beam direction will be affected by the reflections of the signal from scattering objects resulting in sub optimal energy delivery to the receiver.

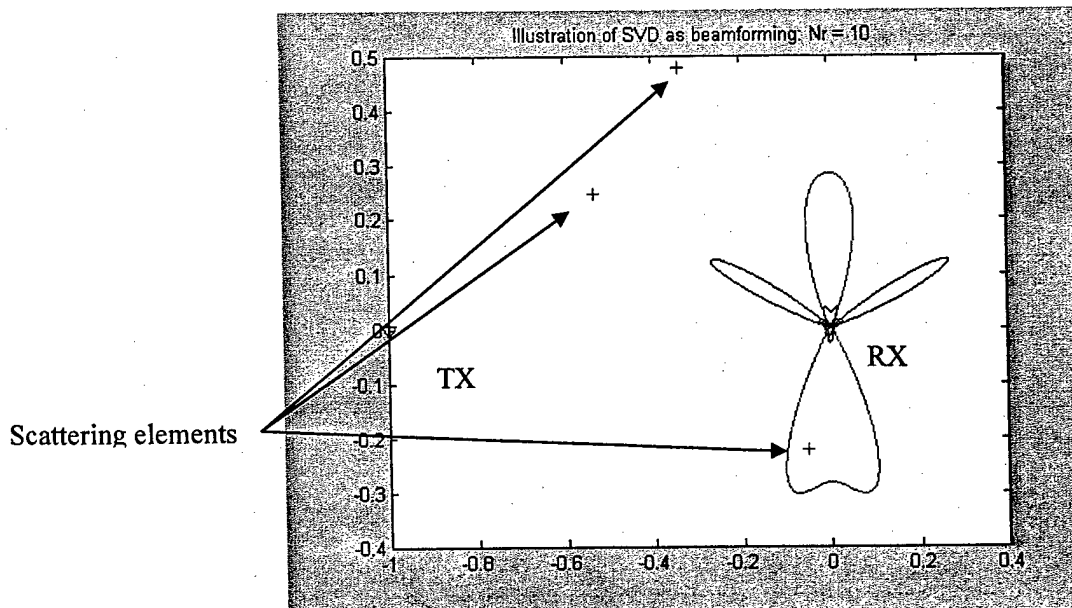


Figure 10, SVD beamforming at the receiver

## 4. Simulation Results

In this section we approach the issue of how to use MIMO transmissions for low probability of detection transmission. Our assumption here is that the enemy is scanning the spectrum and trying to identify if any transmission is taking place. This is typically accomplished by scanning as wide a spectrum as possible and by averaging the received signal over a long period of time.

Our first approach to gaining insight into the LPD properties of MIMO systems was to estimate the SNR required to achieve a capacity of 1 bit per second per Hertz. The study generated five hundred Rayleigh matrix channels and for each one the capacity equation given below was evaluated for the required SNR. The SNR was computed by setting the capacity (the left hand side of the equation) to 1 and solving for  $\rho$ .

$$C = E \left\{ \log_2 \left[ \det \left( I_n + \frac{\rho}{n} H^* H \right) \right] \right\} \text{bits / s / Hz}$$

In the above equation  $C$  is the capacity,  $I_n$  is the  $n \times n$  identity matrix,  $H$  is the Rayleigh channel matrix,  $n$  is the number of transmit antennas, and  $\rho$  is the average signal to noise ratio at each receive branch. The table below shows that at 5% outage, a gain of 22.1 dB is to be had if the number of receiver and transmit antennas is increased from 1 to 8. Another interpretation of the result is that if we want to guarantee that 1bps/Hz can be supported in 95% of all Rayleigh matrix channels encountered, then a 1x1 system needs

an average SNR of 12.8 dB at the receiver, whereas an 8x8 system requires -9.3 dB of averages SNR at the receiver.

MIMO Configuration	Required SNR to achieve 1 bps/Hz of Capacity at 95%
1x1	12.8 dB
2x2	1.2 dB
4x4	-4.9 dB
8x8	-9.3 dB

Table 2. Required SNR to achieve a 95% capacity of 1 bit per second per Hertz (bps/Hz) in Rayliegh channels.

The next metric considered in our studies was a much more conservative metric whereby we measured the ratio of the total energy received at the friendly site to the total energy received at the enemy site. Admittedly this metric is extremely conservative, and provides a upper bound on the LPD performance improvement achievable with MIMO techniques. We define the metric that we term the covert gain as follows:

$$CG = 10 \log \left( \frac{E\{\|H\|_F^2\}}{E\{\|H_e\|_F^2\}} \right)$$

Where  $H$  is the channel between the transmitter and the receiver, and  $H_e$  is the channel between the transmitter and the enemy. The operator  $\|\cdot\|_F^2$  was defined to be the trace of  $H^T H$ . Plotting this metric as a function of the number of antennas at the transmitter and receiver as well as the number of antennas that the enemy has (both with perfect knowledge of  $H_e$  and without) provided us with a great deal of insight regarding the limits of performance improvement for LPD. It is important to note that the covert gain as defined above is an average gain, whereas the results in Table 2 state the 95% capacity gains. The actual gain once an entire system has been constructed (complete with FEC, interleaver, etc.) is expected to be in between these two metrics, but closer to the 95% capacity mark.

Figure 11, shows the plot of the covert gain as a function of the number of transmit and receive antennas assuming that the enemy has only one antenna. In this case, the channel matrix is assumed to be a Rayleigh based channel. The results show significant improvement with the addition of antennas up to approximately 10 elements. The gain thereafter is asymptotic, reaching a limit of approximately 25 dB. To better illustrate this, Figure 12 plots the covert gain as a function of an  $n \times n$  system. In other words, we assume that both the transmitter and the receiver have the same number of antennas. The results clearly illustrate the asymptotic behavior of the system. At this point it is also worth noting that our studies showed that the covert gain improved more with increases in the number of transmit antennas than the number of receive antennas.

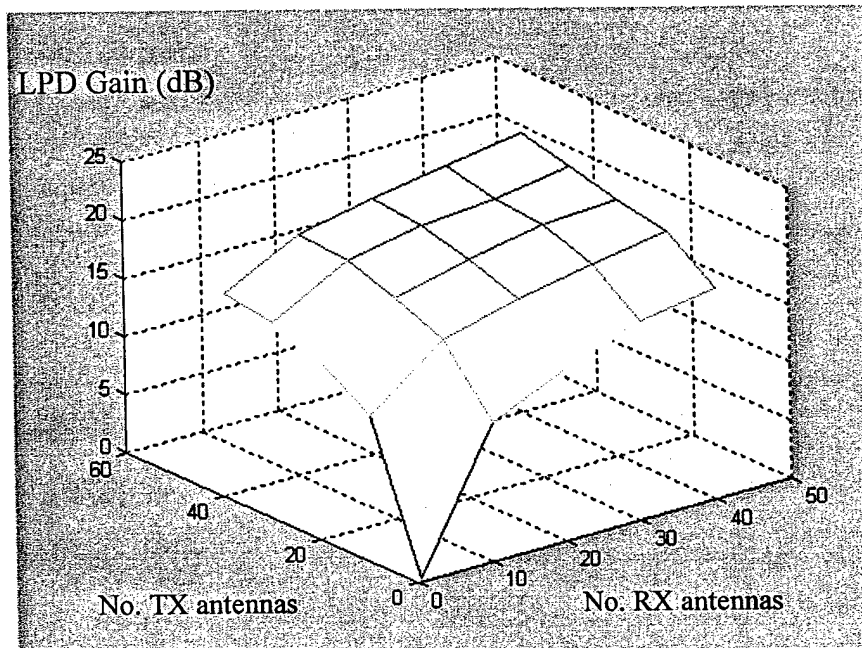


Figure 11, Covert (LPD) gain as a function of the number of transmit and receive antennas. The enemy is assumed to have a single antenna and is assumed to have perfect knowledge of the channel  $H_r$ .

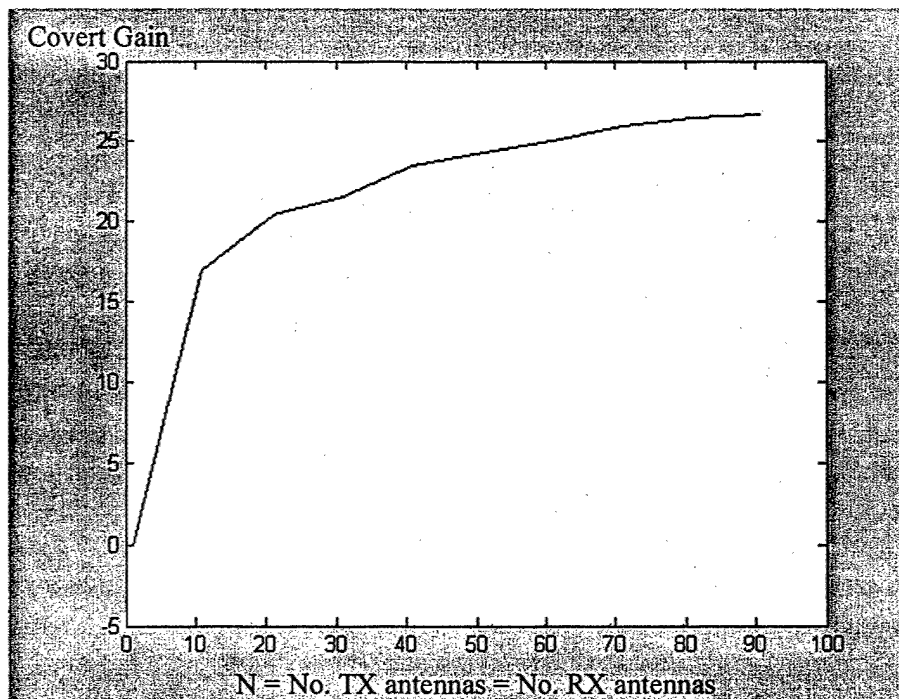


Figure 12. Covert (LPD) gain in dB as a function of the number of antennas at the transmitter and receiver.

The results so far are quite noteworthy, and show the positive and significant impact that MIMO antenna processing can have in improving the LPD properties of the transmission. Studies currently underway show that additional improvement can be achieved if the transmitter is provided with some knowledge of the channel  $H_e$  that exists between the enemy and the transmitter site. An example of such a situation is when a scout, near an enemy site, is trying to communicate with the main forces off in the distance. In this case electromagnetic transmissions from the enemy site can be used to learn some information about the channel. This information can be leveraged to create a pattern that maximizes the energy to the friendly forces, and yet ensures that this transmission is within the null space of the  $H_e$  channel.

## 5. Strategies for AJ and LPI

The strategy for achieving AJ and LPI immunity is somewhat different from that of achieving good LPD protection. LPI is achieved by keeping the enemy system guessing as to the nature of the transmission of the next symbol, packet, or block. Frequency hopped systems achieve this by randomly placing the signal on different carrier frequencies. Direct sequence spread spectrum systems achieve this by randomizing the symbol stream via the use of pseudo random (PN) sequences. In MIMO systems

randomization can be achieved by using different eigenvectors along which the signal can be transmitted. Randomizing the transmissions along the eigenvectors forces the enemy to continuously change the weighting of its receive antennas so as to always ensure that the received signal power is maximized. This assumes that the enemy already knows the eigen modes (eigenvectors) of the matrix  $H_e$ . This is an extremely pessimistic assumption, since it is highly improbable that the enemy can synch up and use the training symbols that the friendlies use to estimate the channel. It requires the enemy to know exactly what the training symbols are which could also be randomized from one transmission to another.

On the other hand, if anti jamming is the main concern, then the MIMO capability at the transmitter and the receiver can be exploited in a different manner. The best immunity to jamming can be achieved by using a non symmetric configuration whereby the receiver is outfitted with more antennas as compared to the transmitter. Running an MMSE based algorithm at the receiver will automatically utilize the additional degrees of freedom at the receiver to effectively null out the jammer or interferer in the spatial domain. This is different from traditional beam nulling since the structure of the channel matrix is an integral part of the nulling process. In the case where this additional degree of freedom is not available, we will incorporate notions similar to those used in frequency hopped spread spectrum systems. In that we look to randomize the signal along the many eigenvectors at the transmitter and then tune the receiver to the particular eigenvector that is being transmitted on. In this situation, since the enemy jammer location is typically fixed the total jammer energy that enters the receiver will be averaged over the eigenvectors used for reception.

The proposed architecture provides several means of improving jamming resistance by utilizing space, time and frequency diversity. Initial simulations indicate that MIMO techniques can drastically improve jamming resistance by forming nulls in the direction of intentional interferers as shown in Figure 13. In this simulation, the system is equipped with four transmit and receive antennas. The plot shows the BER as a function of SNR. Intentional interferes are compared to a benchmark condition of an AWGN channel. The interferer has  $M_{int}$  transmit antennas. The results show the capability of MIMO to cancel an interferer by forming nulls in its direction thus improving the BER performance.

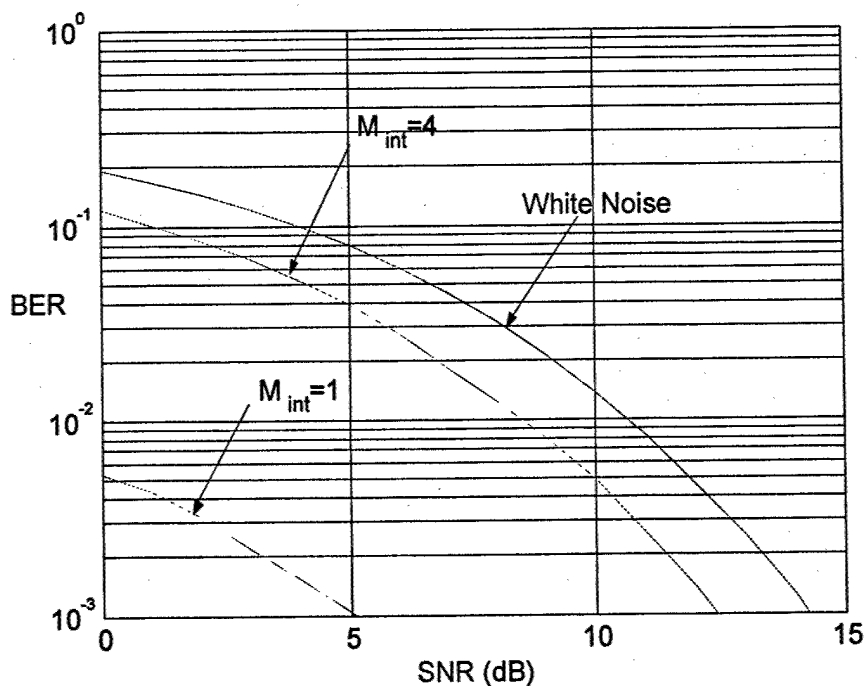


Figure 13 MIMO Interference Nulling

The case for LPI is easily made by realizing that MIMO systems enable a third dimension in the signaling space. So instead of randomizing the signal in time and frequency alone, we can now randomize it in time frequency and space. Moreover, eigen space spreading can be easily combined with conventional frequency hopped or direct sequence spread spectrum techniques. To better illustrate this consider the block diagram of

Figure 2. In the figure each symbol is being sent on a unique OFDM subcarrier and each subcarrier in turn is transmitted along a different eigenvector of the channel. Within the context of a frequency hopped spread spectrum system, then we would not transmit on all OFDM subcarriers within a block, but rather on a subset of them. We would then randomly hop from one subcarrier to the next, while randomly changing the eigen mode along which transmission can take place.

**Combining eigen-space spreading with direct sequence spread spectrum is also possible, as depicted in**

Figure 14. In this approach the data to be transmitted is first spread and scrambled using direct sequence spread spectrum (DSSS) technology. Consecutive data samples are then mapped to the transmit antennas using a spatial randomizer. The spatial randomizer mapping can be changed from one mapping to the next. On each transmit antenna, the data is grouped and then mapped to the OFDM sub-carriers using a second randomizer function which we will refer to as the frequency randomizer. The frequency randomizer function can also be changed from one mapping to the next. Finally the data is simultaneously transmitted in parallel from all antennas. At the receiver, OFDM demodulation is first used to recover the transmitted data on the sub-carriers. OFDM transmission also mitigates the multipath effects. After

parallel to serial conversion of the OFDM sub-carriers by the frequency de-randomizer, the data is presented to the MIMO channel inversion unit to recover the parallel transmitted data streams. Finally, after spatial de-randomization is performed, the data is de-spread and de-scrambled to recover the original bit stream. This approach achieves the same effects as the eigen spreading approach since in this approach data is encoded spatially across the antennas, while in the eigen spreading approach data is encoded spatially across the eigen modes.

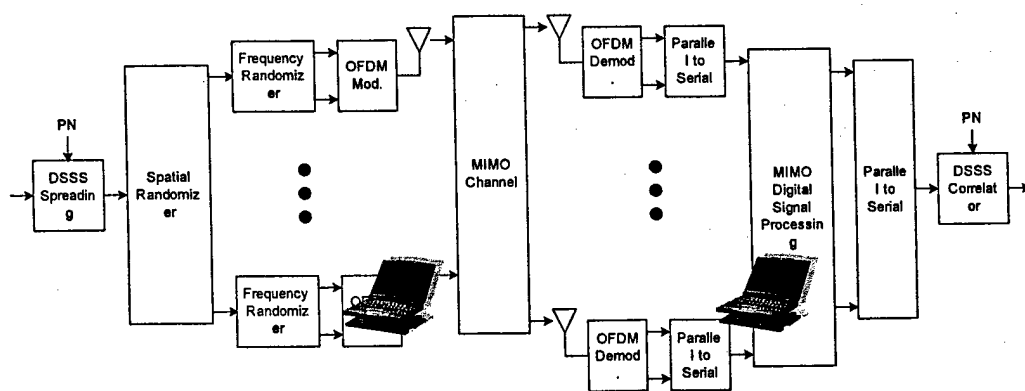


Figure 14, Eigen space spreading combined with Direct sequence spread spectrum.

## Summary & Future Work

The phase 1 effort has shown that significant improvement in LPD and LPI communications can be had by exploiting a third dimension in the signaling space, namely space. The work has laid the foundation for a truly powerful and unique MIMO based LPI/LPD/AJ mode of communications. The basic concepts have been introduced and evaluated by means of semi analytic techniques combined with simulations. What remains is the definition of a signaling structure that would enable synchronization and estimation. The iterative SVD based techniques identified in the phase one work will not have to be integrated with the remainder of the system elements.

The following represents activities that would be addressed as part of a possible phase 2 effort:

- Definition of a complete signaling strategy based on OFDM for the implementation of the eigen vector spreading concepts introduced and exploited in the phase 1 effort

- Quantify gains when DSSS, FHSS, and Eigen space spreading is combined
- Complete sample accurate C model of the candidate signaling strategy
- TX-RX signaling for channel eigen space measurement and identification
- Optimum LPD protection when enemy site is known and is emitting EM energy
- LPD strategy and modeling when no information about enemy location is available
- Implementation of the developed eigen space spreading algorithms onto a real-time platform
- Field testing of the resulting system in realistic combat situations
- Test AJ in the presence of "military grade" jammer
- Measure LPD properties versus a snooping apparatus in use in the field today
- Modification and retuning of the algorithms based on initial field trial results

## References

- [1] G. Foschini, and M. Gans, "On Limits of Wireless Communications in a Fading Environment when Using Multiple Antennas," *Wireless Personal Communications*, vol. 6, no.3, pp. 311-335, March 1998.
- [2] G. Foschini, "Layered Space-Time Architecture for Wireless Communication in a Fading Environment when Using Multi-Element Antennas," *Bell Labs Technical Journal*, vol. 1, no. 2, pp. 41-59, Fall 1996.
- [3] R. Van Nee, and R. Prasad, *OFDM for Wireless Multimedia Communications*. Artech House, 2000.
- [4] K. Sathananthan, C. Tellambura, "Performance analysis of an OFDM system with carrier frequency offset and phase noise," in *Proc. of Vehicular Technology Conference*, vol.4, pp. 2329-2332, 2001.
- [5] M. Ali, J. Gotze, "Efficient implementation of SVD-updating algorithms for subspace tracking," in *Proc. of IEEE Pacific Rim Conference on Communications, Computers and Signal Processing*, vol.2, pp. 366-369, 1993.
- [6] L. Knockaert, B. De Backer, D. De Zutter, "SVD compression, unitary transforms, and computational complexity," *IEEE Transactions on Signal Processing*, vol.47, pp. 2724-2729, Oct 1999.
- [7] G. Burel, "Statistical Analysis of the Smallest Singular value in MIMO Transmission Systems," in *Proc. International conference on signal, speech and image processing*, vol. 1, 2002.
- [8] W. Yan, S. Sun, Z. Lei, "A Low Complexity VBLAST OFDM Detection Algorithm for Wireless LAN Systems," *IEEE Communications Letters*, vol.8, Iss.6, pp. 374- 376, June 2004.
- [9] T. Dahl, N. Christoffersen and D. Gesbert, "Identification of Parallel MIMO Channels in Wireless Communication Using Power Iterations," in *Proc. of 5<sup>th</sup> Nordic Signal Processing Symposium*, vol. 1 ,2002.
- [10] A.A. Saleh, R.A. Valenzuela, "A Statistical Model for Indoor Multipath Propagation," *IEEE Journal on Selected Areas in Communications*, vol. SAC-5, No. 2, pp. 128-137, Feb. 1987.